Quasi-static Component Generation of Guided Waves and Its Applications on Damage Detection

WEIBIN LI, CHANG JIANG, MINGXI DENG
and XINLIN QING

ABSTRACT

Quasi-static component (QSC) generation is a typical nonlinear effect of ultrasonic wave propagation, which can be used for materials characterization with the features of high sensitivity and low attenuative effect (generated QSC pulse's carrier wave frequency is zero). This study presents a novel method for early-stage microdamage detection and localization using QSC generation of ultrasonic guide wave L(0,1) mode propagation in pipes under group velocity mismatching condition. Finite element (FE) model was developed to provide insights on the generation and propagation characteristics of the QSC induced by both the global weak material nonlinearity and local microdamage in metallic pipes. FE analysis verified the L(0,1) mode of the QSC. The cumulation feature of QSC pulse was obtained in terms of the temporal pulse width and the pulse amplitude. A microdamage localization method was pro-posed based on the L(0,1)-QSC mode pair. Experiments were conducted in corrosion-induced aluminum pipes to investigate the QSC pulse signals. The QSC-related nonlinear pulse signals caused by the material nonlinearity and micro-damage were detected and identified. The mode of QSC and feasibility of the proposed micro-damage localization technique were verified. The FE and experimental results demonstrated the basic properties of QSC generation in isotropic metallic pipes and validated potential applications.

Weibin Li, Xinlin Qing, School of Aerospace Engineering, Xiamen University, South Siming Road, 422, Xiamen 361005, China.
Mingxi Deng, College of Aerospace Engineering, Chongqing University, Shazhengjie, 174, Chongqing 400041, China
Chang Jiang, School of Civil, Environmental, and Mining Engineering, University of Adelaide, Adelaide, Australia

INTRODUCTION

Quasi-static component (QSC) generation is a typical nonlinear effect of ultrasonic wave propagation. The relatively low attenuation due to rather low frequency, and high sensitivity to microdamage, make the QSC generation of guided wave (GW) an attractive approach for in-situ inspection of structural parts. The QSC pulse generation was first theoretically studied in isotropic homogenous one-dimensional space by Thurston, Shapiro, and Cantrell [1]. Subsequently, Jacob, Narasimha, Nagy, and Deng studied the QSC generation in solids by theoretical, numerical, and experimental investigations [5]. One of the main findings of these studies in terms of the QSC in solids is that it possesses an envelope-like shape regarding the primary longitudinal tone-burst wave. However, for GW in thin plates or pipes, the dispersion feature of GWs complexes the analysis of QSC generation. Wan, Sun, Gao, and Jiang conducted finite element (FE) simulations and experiments for studying the QSC pulse generated from propagations of different modes of Lamb waves in thin aluminum plates, layered metallic plates, and CFRP laminated plates [6-11]. The QSC generated by Lamb waves was confirmed as S0 mode at near zero frequency for isotropic plates. The temporal waveform and generation efficiency of QSC were investigated and compared with second harmonics. It was found that the QSC generation is cumulative regardless of the synchronism condition as required by the cumulative second harmonic generation and GW mixing. Besides, the generation efficiency of QSC in composite plates is related to the fibre direction, wave mode of primary GW, and the excitation condition.

However, the propagating characteristics of QSC in pipes have yet to be explored and further utilized in practical applications. One significant difference between thin plates and tube-like structures is that the wave energy of the QSC generated in pipes suffers less diffusion than in plates. Due to both the low frequency of the QSC signal and the closed waveguide section, the nonlinear QSC pulse signal can promisingly propagate a longer distance than higher harmonics. Besides, previous studies on the QSC generation mainly employ piezoelectric transducers as signal receiver. In those cases, the QSC signal can only be readily received and extracted when the primary GW acts as the carrier wave of QSC This is one of the main restrictions that limits the mode pair choice and applications of QSC generation. More importantly, although such group velocity matching condition leads to the cumulative magnitude increase of nonlinear signals, it usually disables the microdamage localization when exciting only one fundamental GW and exploiting the correspondingly generated either QSC pulse or higher harmonics.

In this paper, the QSC generation of GWs in pipes is investigated. Importantly, the mode, waveform, and cumulative feature of the QSC are investigated. Furthermore, a novel microdamage localization technique is proposed based on the QSC generation in pipes. The group velocity mismatch between the primary GW and the QSC is exploited as the key feature of the proposed method. Numerical and experimental studies are conducted to validate the proposed technique.

NUMERICAL STUDIES

To study the SC generation in pipes, and further confirm the feasibility of local damage detection, numerical study is conducted firstly. GW of primary L(0,1) mode in the aluminum pipe (2700 kg/m^3 density, 70 GPa Young's modulus and 0.33 Poisson' ratio) is adopted as primary wave to induce the interaction of the ultrasound with the material nonlinearity of the pipe with 3.0mm thickness and 35 mm inner diameter. Accordingly, the phase velocity and group velocity of such pipe are 1574m/s and 2531m/s , respectively. The primary GW mode of L(0,1) at 200kHz is chosen as the fundamental mode, and the SC generated from the GW propagation is expected to be L(0,1) mode at zero frequency, since there exists only L(0,1) and T(0,1) modes at zero frequency, and the latter has no axial displacement.

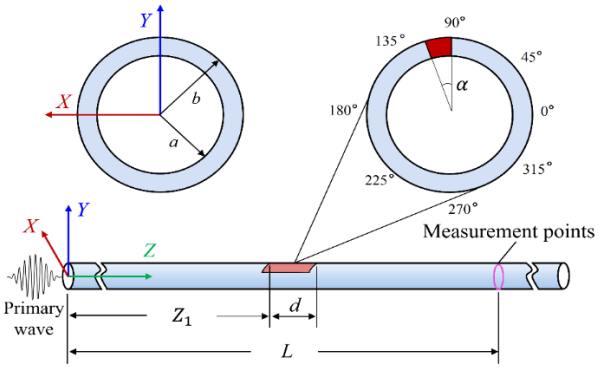

Figure 1. 3D FE model of GW propagation in aluminum pipe with local microdamage.

The 3D FE model is illustrated in Fig. 1. The primary GW is introduced into the pipe by prescribing Hann windowed sinewave displacements on the left end of the pipe. The cycle numbers of the tone-burst signal is 10. The primary wave propagates along the Z direction. For primary L(0,1) mode, the displacement prescribed on the outer boundary at the left end is identical to that prescribed on the inner boundary at the left end in the r direction. This is to excite a pure L(0,1) mode such that other modes are in absence of complicating the subsequent signal analysis. A local microdamage is simulated by scaling up the third-order elastic constants (Murnaghan model: l=-2.5×10^{-11}, m=-3.3×10^{-11}, n=-3.5×10^{-11}, unit: Pa) of the material strain energy function by 1.5 times in the local area. The area is located at $Z_1 = 0.3\text{m}$, and the width is d=0.05m. The central angle of the damage area is denoted by α . For signal receiving, point-probes are placed on the circumferential outer surface of the pipe. The global coordinate of a point position is denoted by (x, y, z). The received displacement in the X, Y, and Z directions are denoted by $U1$, $U2$, and $U3$, respectively. Alternatively, for intuitive understanding of GW propagation, the circumferential and radial displacements described in a cylindrical coordinate system are denoted by U_θ and U_r , respectively. The whole geometry is meshed with structured hex element of size $4.0\times10^{-4}\text{m}$ ($<\lambda/20$, λ is the wavelength of fundamental wave) for suitable

computational accuracy of all the possible secondary GW modes. The time step is 5 $\times 10^{-8}$s.

The mode and cumulative effect of the generated SCs are checked. Fig. 2 shows the received time-domain signals by the point-probes set at 0° at different locations (Fig. 2(a): without local damage; Fig. 2(b): with local damage). As seen in Fig. 2(a), the primary GWs of mode L(0,1) (black line, mainly U_r) is excited into the aluminum pipe. The asymmetric displacements prescribed on the outer and inner boundaries has prevented the generation of L(0,2) to a quite large degree, such that the magnitude of L(0,2) is neglectable. By time-of-flight calculation, the group velocity of the L(0,1) mode is about 2524m/s, which accords with the dispersion curves. On the other hand, due to the global weak material nonlinearity, the red lines (*U3*) show the nonlinear signals obtained by applying the phase-reversal method [1]. The first quasistatic displacement is confirmed as the SC pulse signal. Its group velocity is calculated as about 5071m/s, which accords with the dispersion curve of L(0,1) mode at zero frequency. Since there exists a group velocity mismatch between the primary L(0,1) mode and the SC pulse (L(0,1) mode at nearly zero frequency), the cumulative effect of the SC generation is evidenced by the increase of its pulse width after its amplitude increases to a certain degree. This cumulative phenomenon of SC pulse is similar to that of GW propagations in plates [9-11].

For the local damage case (See Fig. 2(b)), due to the greater third-order elastic constants, there is a local pulse vibration (at about 3×10^{-4}s) after the first quasistatic displacement pulse (at about 2×10^{-4}s). It increases the amplitude of the SC signal to a greater level. This is because that, the local micro-damage is acting as a wave energy transfer station, where the power of primary GW transfers into the nonlinear signals. Consequently, due to the group velocity mismatch, the newly generated SC pulse signal is propagating faster than the primary L(0,1) mode, and slower than the SC pulse signal induced by the global weak material nonlinearity. Hence, this local vibration occurring at about t=3×10^{-4}s can be a promising index to indicate the location of the microdamage.

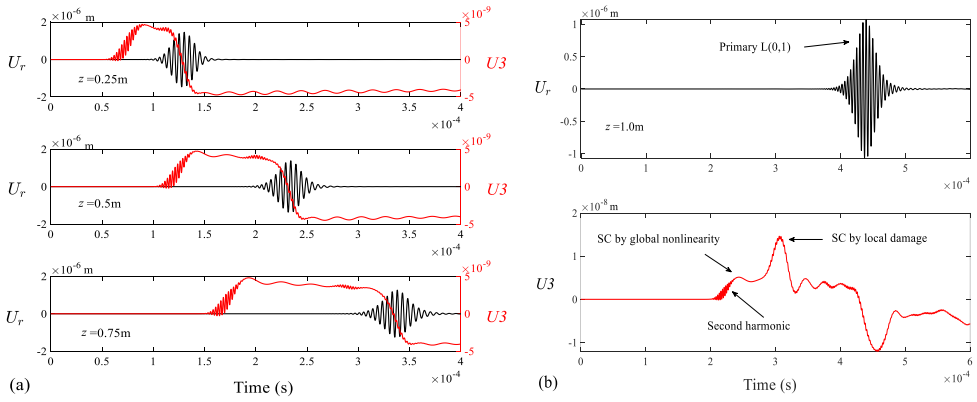

Figure 2. Time domain signals of primary L(0,1) GW received in r direction (black lines) and nonlinear signals received in Z direction (red lines): (a) without local damage, (b) with a local damage.

EXPERIMENTS

The four samples used in the experiments are aluminum pipes with the same outer and inner radii as in the FE simulations ($a=17.5\text{mm}$, $b=19\text{mm}$). The lengths are 1.5m. One pipe was left intact (#0), and others were artificially damaged. Corrosion, as one of the main damage forms of metallic materials, was made in a local area on the pipes. The selected corrosion reagents were high-concentrated Keller reagent and analytical hydrochloric acid. There are three corrosion samples. The corrosion of the specimens was carried out in a fume hood with double-sided sponge tape applied to the surface of the specimen to form a square groove preventing the spreading of the corrosion solution. Firstly, we used the Keller reagent on the designed surface areas for 30 seconds, then added concentrated hydrochloric acid to the same surface locations (Z_1 =0.3m, d=0.05m, $\alpha=360°$) of two pipes for 30s (#1), and 60s (#2), respectively, to generate corrosion-related micro-defects of different degrees. One pipe was corrosion processed for 60s but at a different location (#3: Z_1=0.65m, d=0.05m, $\alpha=360°$). The measuring process was performed using the experimental setup shown in Fig. 3. The excitation tone-burst signal was generated by a NI signal generation module, then amplified by a high-power amplifier with 150V peak-to-peak voltage. A load resistance 50 Ω was used for impedance matching. An oscilloscope was used to observe the input signal. Eight rectangular PZTs (Dimensions: 5.0 mm×6.0 mm×1.0mm) were attached around the left end outer surface using conductive epoxy for the wave generation in the pipe. The propagating tone-burst wave in the pipe was then measured using a 3D laser Doppler scanning vibrometer and acquisition system. The measurement area was painted with reflective coating. The recorded signals were averaged 1500 times to improve the signal-to-noise ratio. The sampling frequency of acquisition was set as 2.56 MHz with 390.6 ns sampling resolution, and a low-pass filter was applied with upper limit of 600 kHz. Each measuring process was repeated three times to determine the uncertainty of the experimental results.

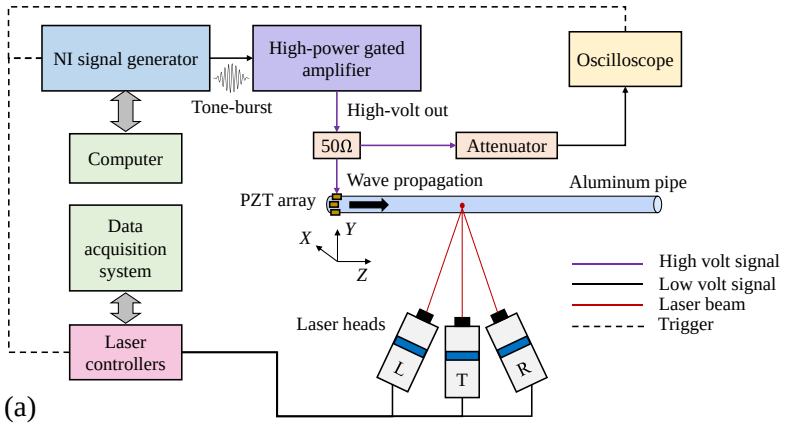

(a)

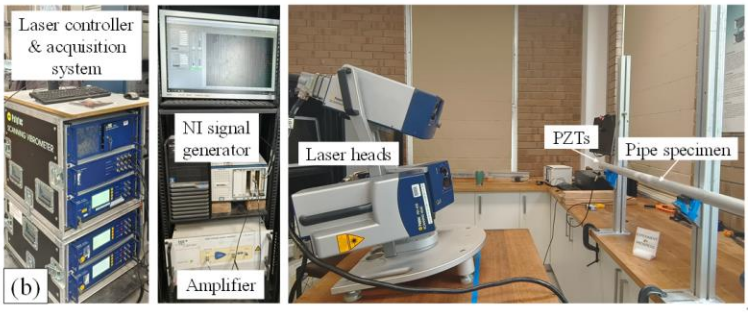

Figure 3. Experimental setup: (a) system diagram, (b) physical pictures of key parts.

To observe the secondary wave field, the phase-reversal method conducted for the FE simulation was also applied in the experiments to counteract the primary waves and double the magnitude of the nonlinear waves. Specifically, based on the numerical results in Sections 2, the SC pulse vibration is confirmed to be polarized in the axial *Z* direction. Thus, we focus on the signal processing of axial displacement components obtained by the 3D laser system. Typical received time-domain signals in the corrosion damaged pipes #1, #2, and #3 after applying the phase-reversal processing is shown in Fig. 4(a). It is found that the nonlinear signals contain both the global material nonlinearity-induced SC and the local corrosion damage-induced SC. The former is received by the laser system (picking point: z=1.0m) at about 2.0×10^{-4}s for all the pipes. For the corrosion damage-induced SC, the local DC vibration at around 3.2×10^{-4}s is not quite obvious for pipe #1, which was suffered to the artificial corrosion processing for only 30s. However, there exists a significant DC displacement at around 3.2×10^{-4}s and 3.8×10^{-4}s for pipe #2 and pipe #3, respectively. This is mainly due to that the 60s corrosion process has resulted in the large increase of material nonlinearity at the corrosion areas of the two pipes. While the primary L(0,1) GW propagates through the corrosion areas, the fundamental GW power flows into the SC pulse signal.

Furthermore, by time-frequency analysis, Fig. 4(b) shows the power spectra of the nonlinear signals in dB scale. The main frequencies of these signals are near zero, and the local damages lead to three power peaks in the spectra. The time-of-flight for these three local DC displacement shifts caused by the local corrosion damages can be extracted and used for centre damage location estimation by a set of equations

$$\begin{aligned} &c_g^{L(0,1)} \cdot t_1 + c_g^{SC} \cdot t_2 = L + W, \\ &t_1 + t_2 = TOF, \\ &Z_c = c_g^{L(0,1)} \cdot t_1, \end{aligned} \tag{1}$$

where c_g is the group velocity, t_1 and t_2 are time periods for the fundament wave propagates to the microdamage area and for the induced SC arrives at the receivers, respectively, *TOF* denotes the arrival time of the power peak in the time-frequency spectrum, and Z_c is the estimated centre location of the local damage, *L* is the total

propagation distance of the tone burst primary guided wave, and *W* is the length of guided wave packet.

It is noted that the proposed method cannot perform an assessment of the damage location in the circumferential direction of the pipe. This has been expected in Section 2 by the FE results. The aluminum pipe specimens are of relatively small radius, and the path length difference of GW propagation by the circumferential receiving points at z=1.0m is negligible. Also, the proposed method is not currently feasible to achieve the localization of multiple micro-damages in a pipe at the same time. Besides, it should be noted that the degree of group velocity mismatch is essential to the proposed method. With greater group velocity mismatch, the localization resolution is supposed to be more accurate, and the detectable damage location range is expected to be wider as well.

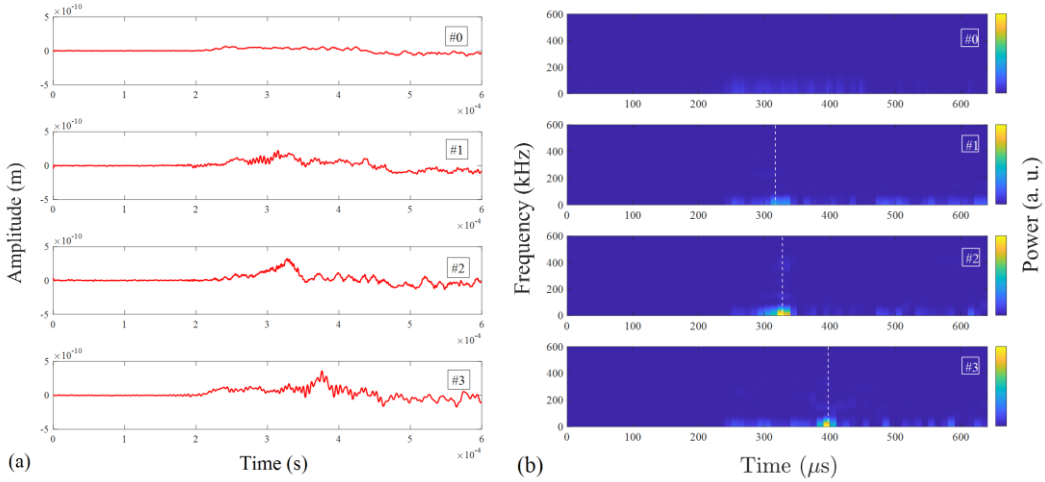

Figure 4. (a) Time domain signals and (b) corresponding time-frequency domain analysis of nonlinear signals after phase-reversal processing.

CONCLUSIONS

In this paper, the SC generation from the propagation of guided waves in isotropic aluminum pipes has been investigated. The mode, waveform, along with the cumulative effect of the generated SCs have been confirmed. The SC pulse signals have been confirmed as zero-frequency L(0,1) mode with only uniform axial displacement, and the group velocity mismatch condition has been found as the factor that influence the pulse width increase of SC signal. Besides, a novel local micro-damage localization method involving only a single one-way primary wave propagation has been proposed. The method has been validated by experiments using L(0,1)-SC mode pair with group velocity mismatch and 3D laser measuring system in corrosion aluminum pipes. Experimental results show good agreement with the numerical results, and indicate promising applications of the method in early stage microdamage detection, localization, and monitoring for key structural parts in many fields.

REFERENCES

1. Thurston, R. N. and M. J. Shapiro. 1967. “Interpretation of Ultrasonic Experiments on Finite-amplitude Wave,” *J. Acous. Soc. Am.,* 41:1112-1120.
2. Cantrell, J. H. 1984. “Acoustic-radiation Stress in Solids. I. Theory”, *Phys. Rew. B.,* 30: 3214.
3. Deng, M. 2008. “Second-harmonic Generation of Ultrasonic Guided Wave Propagation in an Anisotropic Solid Plate”, *Appl. Phys. Lett.*, 92: 111910.
4. Nagy, P. B., J. Qu, L. J. Jacobs. 2013. “Finite-size Effects on the Quasistatic Displacement Pulse in a Solid Specimen with Quadratic Nonlinearity”, *J. Acous. Soc. Am.* 134:1760-1774.
5. Deng, M. 2020. “An Experimental Approach for Detection of the Acoustic Radiation Induced Static Component in Solids”, *Chin. Phys. Lett.,* 37:074301.
6. Wan, X., P. W. Tse, X. Zhang, et al., 2018. “Numerical Study on Static Component Generation from the Primary Lamb Waves Propagating in a Plate with Nonlinearity”, *Smart Mater. Struct.,* 27:045006.
7. Sun, X., G. Shui, Y. Zhao, W. Liu, N. Hu and M. Deng. 2020. “Evaluation of Early Stage Local Plastic Damage Induced by Bending using Quasi-static Component of Lamb Waves”, *NDT & E Inter.,* 116:102332.
8. Gao, G., H. Chen, N. Hu and M. Deng. 2021. “Experimental Observation of Static Component Generation by Lamb Wave Propagation in an Elastic Plate”, *Ultrasonics*, 117:106537.
9. Jiang, C., W. Li, M. Deng and C. Ng C. 2021. “Static Component Generation and Measurement of Nonlinear Guided Waves with Group Velocity Mismatch”, *JASA Express Lett.,* 1:055601.
10. Jiang, C., W. Li, M. Deng and C. Ng. 2022. “Quasistatic Pulse Generation of Ultrasonic Guided Waves Propagation in Composites”, *J. Sound Vib.,* 524:116764.
11. Jiang, C., C. Zhang, W. Li, M. Deng and C. Ng. 2022. “Assessment of Damage in Composites Using Static Component Generation of Ultrasonic Guided Waves”, *Smart Mater.Struct.,* 31:045025.